NASA Contractor Report 4439

Boundary-Layer Receptivity Due to Distributed Surface Imperfections of a Deterministic or Random Nature

Meelan Choudhari

CONTRACT NAS1-18240
MAY 1992

NASA Contractor Report 4439

Boundary-Layer Receptivity Due to Distributed Surface Imperfections of a Deterministic or Random Nature

Meelan Choudhari
High Technology Corporation
Hampton, Virginia

Prepared for
Langley Research Center
under Contract NAS1-18240

National Aeronautics and
Space Administration

Office of Management

Scientific and Technical
Information Program

1992

Boundary-Layer Receptivity due to Distributed Surface Imperfections of a Deterministic or Random Nature

Meelan Choudhari
High Technology Corporation
Hampton, VA 23666.

Abstract

Acoustic receptivity of a Blasius boundary layer in the presence of distributed surface irregularities is investigated analytically. It is shown that, out of the entire spatial spectrum of the surface irregularities, only a small band of Fourier components can lead to an efficient conversion of the acoustic input at any given frequency to an unstable eigenmode of the boundary layer flow. The location, and width, of this most receptive band of wavenumbers corresponds to a relative detuning of $O(R_{l.b.}^{-3/8})$ with respect to the lower-neutral instability wavenumber at the frequency under consideration, $R_{l.b.}$ being the Reynolds number based on a typical boundary-layer thickness at the lower branch of the neutral stability curve. Surface imperfections in the form of discrete mode waviness in this range of wavenumbers lead to initial instability amplitudes which are $O(R_{l.b.}^{3/8})$ larger than those caused by a single, isolated roughness element. In contrast, irregularities with a continuous spatial spectrum produce much smaller instability amplitudes, even compared to the isolated case, since the increase due to the resonant nature of the response is more than compensated for by the asymptotically small band-width of the receptivity process. Analytical expressions for the maximum possible instability amplitudes, as well as their expectation for an ensemble of statistically irregular surfaces with random phase distributions, are also presented.

1 Introduction

The purpose behind this paper is to present some theoretical results concerning the acoustic receptivity of a boundary layer flow due to distributed surface imperfections, which can be either deterministic or random in terms of their origin. Such imperfections may arise due to a variety of causes, ranging from manufacturing defects or structural joints to operational factors, such as paint erosion, insect debris and ice accretion, etc. [1]. Of the many ways they have been known to affect the transition to turbulence, inducement of receptivity is a major one when the maximum height of these irregularities is small.

The generation of Tollmien-Schlichting (henceforth T-S) instabilities in low-speed boundary layers via the interaction of free-stream sound with a local surface distortion was first explained by Goldstein [2] and Ruban [3] in 1985. They showed that receptivity in this case can be attributed to the fact that the unsteady scattered field produced by this interaction inherits its temporal scale from the free-stream disturbance but its spatial scales from the shorter surface irregularity, thereby acquiring a Fourier spectrum that overlaps with the T-S wave. Following this fundamental breakthrough, a variety of other localized receptivity problems were studied by other investigators, and examples of these can be found in the proceedings [4] and [5].

Receptivity due to distributed waviness of the surface was studied by Crouch [6] [7]; however, the conclusions of these two references concerning the magnitude of receptivity are contradictory to each other. Furthermore, the prediction technique used therein appears to be more suitable for distributions of surface nonuniformities which are homogeneous in the flow direction and only involve a finite number of (discrete) Fourier modes. On the other hand, Choudhari and Streett [8] had shown how generation of instabilities via distributed regions of surface inhomogeneities could, in general, be predicted by a relatively simple extension of the localized receptivity results. This extension is based on treating the receptivity in a region of large streamwise extent as a sum of the contributions from its constituent sub-domains of infinitesimal size, in each of which localized receptivity analysis becomes applicable. The same idea was used originally by Tam [9] in an attempt to predict the direct excitation of instability waves in the absence of any non-uniformities on the surface. The advantages of this technique include its applicability to arbitrary distributions of surface inhomogeneities, and its simplicity in leading to a first order ordinary differential equation for the amplitude of the instability wave at any given frequency. The latter, as demonstrated in this paper, facilitates a further analytical treatment of the distributed

receptivity problem, thereby yielding closed form expressions for the generated instability motion and also providing a clearer interpretation of the physics involved.

The receptivity to a single frequency acoustic disturbance in the presence of surface imperfections of known shape and distribution is considered first in Section 2.2 below, following a brief discussion of the general procedure for solving receptivity problems involving weak surface inhomogeneities; a more detailed discussion of the background analysis can be found in Refs. [8] and [10]. Although the classical Orr-Sommerfeld framework has been utilized as the basis throughout, a similar treatment could also have been applied to the problem using a purely asymptotic theory. The results obtained in Section 2.2 for the deterministic problem are used as the building block in Section 2.3 for analyzing receptivity due to a random roughness distribution with a specified power spectral density. Numerical verification of the theoretical results is also considered.

2 Receptivity Analysis for Distributed Surface Inhomogeneities

2.1 Background and Problem Formulation

Consider the two-dimensional flow over a slightly rough surface that is nominally flat and aligned with an incompressible free-stream with mean speed U^*_∞, plus time-harmonic fluctuations having frequency ω^*, and amplitude u^*_{ac}, such that $\epsilon_{fs} = u^*_{ac}/U^*_\infty << 1$ (Fig. 1). The maximum perturbation in the surface height $h^*_w(x^*)$ with respect to the mean position $y^* = 0$ is also assumed to be sufficiently small compared to the mean boundary-layer thickness ($\epsilon_w = (h^*_w/\delta^*)_{max.} << 1$) so that the flow everywhere can be expanded as a regular perturbation series in terms of the amplitude parameters ϵ_w and ϵ_{fs}. As described below, each term in this perturbation series turns out to involve a different combination of spatial and temporal scales, and the objective from the standpoint of receptivity is then to determine the first term which contains the desired combination of scales, i.e., one that overlaps with the local instability wave. Of course, in order to determine this term with a given order of accuracy in terms of Reynolds number effects, one needs to know all the previous terms also to the same order of accuracy.

It should be obvious that the zeroth order term corresponds to the Blasius streamfunction for the mean boundary-layer flow over a flat surface, while the $O(\epsilon_{fs})$ perturbation, corresponding to the unsteady signature of the acoustic free-stream fluctuation within this boundary layer, is given by the generalized Stokes-wave solution obtained in [11]. The $O(\epsilon_w)$ perturbation, corresponding to the steady but short-scale disturbance due to variations in the surface geometry, satisfies the parallel flow

equations up to $O(R^{-3/4}\,log\,R)$ on a local basis, although the large-scale modulation due to the weak growth of the Blasius boundary layer also comes into play, depending on the streamwise extent of the region of imperfections. Note that R denotes the Reynolds number based on the boundary-layer scale and is defined as $R = \sqrt{Re_{x^*}}$, Re_{x^*} being the Reynolds number based on the distance from the leading edge.

The first term in the amplitude expansion which possesses both unsteadiness and short spatial scales, and hence is the object of the receptivity calculation, corresponds to the $O(\epsilon_w \epsilon_{fs})$ term arising from a quadratic coupling between the unsteady free-stream and steady surface disturbances. Physically, it represents the unsteady field produced by the interaction of the $O(\epsilon_{fs})$ Stokes shear wave with the $O(\epsilon_w)$ mean flow perturbation, and by its direct scattering due to the $O(\epsilon_w)$ perturbation in the surface height. Within the "geometrical optics" approximation, this scattered field is governed by the unsteady linear disturbance equations for a locally parallel mean flow, along with inhomogeneous terms in the differential equations themselves and in the boundary conditions as well, in view of the two different mechannisms for scattering as mentioned above. Again, non-parallel effects will need to be considered if propagation distances become comparable to the body-length scale. However, subsequent analysis will show that most of the receptivity is actually concentrated in a region of much smaller streamwise dimension and hence, a prediction based on the parallel flow equations is sufficient, at least to the leading order of approximation in terms of the Reynolds number.

Both the mean flow perturbation and the unsteady scattered field, thus, satisfy the quasi-parallel disturbance equations, and therefore can be solved on a local basis by reducing these partial differential equations to ordinary ones through the use of a Fourier transform in the streamwise direction. The equations in the transform space can be solved either in closed form, via a systematic but multi-layer expansion in terms of the Reynolds number [2-5], or numerically by using the Orr-Sommerfeld equation as a non-asymptotic but composite approximation [4-8]. In either case, the locally generated instability wave can be isolated as the residue contribution corresponding to a pole singularity of the inverse Fourier integral for the unsteady scattered field. This residue contribution is linear in terms of the local perturbation to the mean surface-height, with a coefficient function, Λ_u, that characterizes the efficiency of the local receptivity process. The T-S fluctuations produced locally, i.e., in each infinitesimal subregion, propagate independently of the instability motion generated elsewhere, with their amplitude and phase variation being determined by the T-S wavenumber as a function of R. The

total instability amplitude at any location is then given by the integral over the contributions from all sources upstream of this location[8,10]

$$\frac{u^*_{TS}}{u^*_{ac}} = \sqrt{\frac{2}{\pi}}\, E_u(Y;\, R)\, e^{i[\Theta_{TS}(R)-\omega t]} \int^{R} \Lambda_u(R_s)\, h_w(R_s)\, e^{-i\Theta_{TS}(R_s)}\, H(R-R_s)\, dR_s, \qquad (2.1a)$$

where u^*_{TS} denotes the streamwise velocity fluctuation associated with the T-S motion, E_u is the T-S eigenfunction for this quantity, normalized to have a maximum magnitude of unity across the boundary layer, and Θ_{TS} is the spatial phase of the T-S wave

$$\Theta_{TS}(R) = 2\int^{R} \alpha_{TS}(R)\, dR \ . \qquad (2.1b)$$

The quantity $h_w(x^*)$ is the local perturbation in the surface height, nondimensionalized by the slowly varying length scale $x^* Re_{x^*}^{-1/2}$, and Λ_u is the efficiency function obtained from localized receptivity analysis. One should note that the streamwise variations of the eigenfunction E_u, wavenumber α_{TS}, and efficiency factor Λ_u are much slower than those of the instability phase Θ_{TS} and the surface-height function h_w; thus we have $|\frac{1}{\Lambda_u}\frac{d\Lambda_u}{dR}| << |\frac{1}{\Theta_{TS}}\frac{d\Theta_{TS}}{dR}|$, etc. In Fig. 2, we have shown the Reynolds number dependence of the magnitude of Λ_u for selected values of the nondimensional frequency parameter $f_0 = 10^6 \times \omega^* \nu^* / U^{*2}_{\infty}$.

By differentiating with respect to R and invoking the quasi-parallel approximation, Eq. (2.1a) can also be converted to a wave amplitude equation similar to that obtained by Tam [9],

$$\frac{du^*_{TS}}{dR} = i\,\frac{d\Theta_{TS}}{dR}\, u^*_{TS} + \sqrt{\frac{2}{\pi}}\,\Lambda_u\ h_w\,, \qquad (2.2)$$

where, for simplicity, we have omitted the Y-dependence of the disturbance motion, and from now on, u^*_{TS} will denote simply the maximum of the streamwise velocity perturbation at each streamwise location. The homogeneous solution to this amplitude equation corresponds to the T-S wave, which is excited every time the local spectrum of the geometry function h_w overlaps with the T-S wavenumber. As seen from Eq. (2.2), when the receptivity occurs continuously over a large number of instability wavelengths, the change in the wave amplitude at any station is a combined outcome of the local amplification of the instability waves generated upstream of the present location and the external input due to local receptivity. As discussed in Refs. [9] and [10], the external input dominates the initial development of the instability amplitude; however, after u^*_{TS} becomes sufficiently large in magnitude, the amplitude evolution curve asymptotes to that of a pure T-S wave eigensolution. Note also that, as a result of the distributed receptivity process, the location of stationary (i.e., maximum) amplitude

does not correspond to the theoretical upper-branch location $R_{u.b.}$. However, the shift is asymptotically small, and one may, therefore, measure the generated instability motion in terms of its amplitude at the upper-branch location itself. The intrinsic receptivity can be gauged by dividing the nondimensional amplitude $u^*_{TS}(R = R_{u.b.})/u^*_{ac}$ by the amplification ratio between the two neutral locations, which leads to an "effective coupling coefficient", C, indicating the effective instability amplitude at the beginning of the linear amplification stage. A coupling coefficient[9] basically relates the output of the receptivity process, i.e., the amplitude of the generated instability wave, to its input, i.e., the free-stream disturbance amplitude, and the measure C is the local coupling coefficient for an equivalent, but ficticious, localized mechanism that has all its receptivity lumped together at the lower-branch station $R = R_{l.b.}$. Approximate analytical expressions for the effective coupling coefficient for different types of geometries are derived in Sections 2.2 and 2.3 below.

2.2 Receptivity due to a single-mode surface waviness

Since any spatially homogeneous distribution of roughness elements can be examined in terms of its individual Fourier components, we first consider geometries of the form

$$h_w(R) = \frac{R_{h_0}}{R} e^{i\Theta_w(R)}, \text{ where } \Theta_w = \int_{R_{l.b.}}^{R} 2\alpha_w(R)\, dR + \phi_0, \;\; \alpha_w(R) = 2\pi \frac{R}{R_{\lambda^*_w}} \;, \tag{2.3}$$

corresponding to a surface with single-mode waviness of constant nondimensional amplitude R_{h_0}. Note that R_{h_0} is the Reynolds number based on the free-stream speed U^*_∞ and the dimensional amplitude of the surface-height perturbation h^*_0. Similarly, $R_{\lambda^*_w}$ is the Reynolds number based on the constant dimensional wavelength $\lambda^*_w (= 2\pi/\alpha^*_w)$ of the surface undulations, while α_w denotes the dimensionless wavenumber based on the slowly-varying, local length scale, $x^* Re_{x^*}^{-1/2}$. The integral solution (2.1a) now becomes

$$\frac{u^*_{TS}}{u^*_{ac}} = \sqrt{\frac{2}{\pi}}\, R_{h_0}\, e^{i\Theta_{TS}(R) + i\phi_0 - i\omega t} \int^{R} \frac{\Lambda_u(R_s)}{R_s}\, e^{i[\Theta_w(R_s) - \Theta_{TS}(R_s)]}\, dR_s. \tag{2.4}$$

Since the efficiency function Λ_u varies slowly with the integration variable R_s, the integrand in (2.4) is nearly oscillatory if the wavenumber of the surface undulations α_w differs from the local instability wavenumber α_{TS} by an $O(1)$ magnitude. Then contributions from the neighbouring surface locations corresponding to the out-of-phase elements during each cycle of oscillation nearly cancel each other, and the integral becomes end-point dominated. This implies that the disturbance amplitudes will retain the the same order of magnitude throughout the region of waviness.

2.2.1 Waviness synchronized with the neutral instability motion

A sustained generation of instabilities will occur only if $\alpha_w \approx \alpha_{TS}$, corresponding to a nearly synchronous variation of the forcing phase Θ_w and the eigenmode phase Θ_{TS}, which leads to a mutual reinforcement of the contributions to the integral in (2.4) from adjacent surface locations. Of course, since the instability wavenumber varies slowly with distance along the surface, such a resonance is necessarily localized in space, and the extent of this localization determines how large the distributed receptivity is, when compared to the receptivity induced by a single, isolated roughness element. Since the instability wavenumber is complex, in general, the condition of perfect local resonance requires that

$$\alpha_w^* = \alpha_{TS}^*(R_{l.b.}) \text{ or } \alpha_w^* = \alpha_{TS}^*(R_{u.b.}), \qquad (2.5a,b)$$

where the asterisk denotes dimensional quantities, and subscripts $l.b.$ and $u.b.$ represent lower and upper branches of the neutral stability curve, respectively. When (2.5a) or (2.5b) is satisfied, the exponent in the integrand of (2.4) has a saddle point at the respective neutral location, with the real R axis corresponding to a path of descent in case of (2.5a), and a path of ascent when (2.5b) is true. The latter case is, of course, of little practical interest, and will not be discussed here.

The presence of a saddle point at $R = R_{l.b.}$ implies that the importance of the local contribution to the effective coupling coefficient diminishes rapidly with distance away from the lower branch location. Applying the steepest descent method yields the following approximation for the effective coupling coefficient

$$C_{p.s.} = \frac{R_{h_0}}{R_{l.b.}} \sqrt{\frac{2}{iD_\alpha}}\, \Lambda_u(R_{l.b.})\, e^{i\phi_0} \ , \ D_\alpha = \alpha_w' - \alpha_{TS}' \ , \qquad (2.6)$$

where the suffix $p.s.$ indicates that the condition (2.5a) for perfect synchronization is satisfied, and the primes denote derivatives with respect to R, evaluated at the neutral location $R = R_{l.b.}$. The dispersion factor D_α, which is simply $Re_{x^*} x^{*2} \frac{d\alpha_{TS}^*}{dx^*}|_{x^*=x_{l.b.}^*}$ in dimensional terms, controls the rate at which the phase of the natural response becomes uncorrelated with the surface geometry as one moves away from the resonance location. Asymptotically, the magnitude of this factor is of $O(R_{l.b.}^{-5/4})$, and therefore the length of the resonance region corresponds to $\Delta R = O(R_{l.b.}^{5/8})$, or in physical terms, $\Delta x^* = O(x_{l.b.}^* R_{l.b.}^{-3/8})$, which is of the same order as the geometric mean of the distance from the leading edge and the instability wavelength at the lower branch location. This shows that that the synchronized surface waviness will lead to instability amplitudes which are larger than those produced by an isolated surface protuberance by a factor of $O(R_{l.b.}^{3/8})$. This simple analytical result confirms,

as well as explains, the more recent computations of Crouch (Ref. 7) where he found the distributed receptivity to be "two orders of magnitude" larger than that due to an isolated roughness element, as against his earlier findings (Ref. 6) that the receptivity is comparable in both cases. Finally, since in practice, the imaginary part of D_α is larger than its real part at all frequencies of interest, the dispersion effect which leads to the detuning of the forcing $\Theta_w(R)$ with respect to $\Theta_{TS}(R)$ is caused more by the variation in the instability growth-rate, than by a variation in the instability phase-speed near $R = R_{l.b.}$.

It is equally instructive to consider the single mode waviness problem using Tam's wave amplitude equation (2.2), which is physically analogous to the second order equation obtained for a forced oscillator with slowly-varying parameters, except that the oscillator motion usually involves a zero or positive damping. Both linear and nonlinear problems of this type have received, and continue to receive, ample attention from applied mathematicians over the years as evidenced from the various citations in a recent review by Kevorkian [12], which appear to have begun with Ref. [13] in 1971. Hence, only a brief sketch of the solution to (2.2) is given here. A reader interested only in receptivity may also find some supplemental discussion, especially related to the appropriate initial condition for (2.2), as well as the numerical results for the case of wall-suction induced receptivity, in Ref. [10].

Basically, the total disturbance amplitude consists of a superposition of the particular solution,

$$u_p^* = u_{ac}^* \frac{1}{i\sqrt{2\pi}} \frac{R_{h_0}}{R_{l.b.}} \frac{\Lambda_u(R_{l.b.})}{\alpha_w(R_{l.b.}) - \alpha_{TS}(R_{l.b.})} e^{i\Theta_w(R)} , \tag{2.7a}$$

and a constant multiple of the homogeneous solution,

$$u_h^* = u_{ac}^* e^{i\Theta_{TS}(R)} . \tag{2.7b}$$

If $\alpha_w/\alpha_{TS} - 1 = O(1)$ everywhere, then the two solutions (2.7a) and (2.7b) remain decoupled, i.e., linearly independent, everywhere, and imposing an initial condition corresponding to zero initial instability amplitude forces the coefficient of the homogeneous solution to be zero identically. On the other hand, when the resonance condition (2.5a) is satisfied, the particular solution becomes singular at $R = R_{l.b.}$, reflecting the fact that the particular and homogeneous solutions are linearly dependent in the vicinity of this location, and, therefore, the decomposition of the total solution into (2.7a) and (2.7b) is invalid.

A separate, inner expansion becomes necessary for $(R - R_{l.b.})/R_{l.b.} = O(R_{l.b.}^{-3/8})$, wherein both $\alpha_w(R)$ and $\alpha_{TS}(R)$ can be approximated by their respective linear Taylor-series approximations centered on

the resonance location, $R = R_{l.b.}$. Expressing the coupling coefficient u^*_{TS}/u^*_{ac} in the inner region as the product of a rapidly-varying component $e^{2i\alpha_{l.b.}(R-R_{l.b.})}$, which incorporates the phase synchronization with the local instability motion, with an amplitude function $A(R)$ that varies on the inner length-scale, we obtain the amplitude evolution equation

$$\frac{dA}{dR} = 2i\alpha'_{TS}(R - R_{l.b.})A + i\sqrt{\frac{2}{\pi}}\,\frac{R_{h_0}}{R_{l.b.}}\,\alpha'_w\,\Lambda_u(R_{l.b.})\,e^{i\phi_0 + i\alpha'_w(R-R_{l.b.})^2}, \tag{2.8}$$

where, for brevity, we have avoided introducing a specific coordinate just for the inner region. The solution to (2.8),

$$A(R) = A_{l.b.}e^{i\alpha'_{TS}(R-R_{l.b.})^2} + \sqrt{\frac{2}{\pi}}\,\frac{R_{h_0}}{R_{l.b.}}\,\Lambda_u(R_{l.b.})\,e^{i\alpha'_{TS}(R-R_{l.b.})^2}\int_{R_{l.b.}}^{R} e^{i\phi_0 + iD_\alpha(R_s-R_{l.b.})^2}dR_s\,, \tag{2.9}$$

matches the particular solution (2.7a) sufficiently far upstream, provided

$$A_{l.b.} = \frac{R_{h_0}}{R_{l.b.}}\,\frac{\Lambda_u(R_{l.b.})}{\sqrt{2iD_\alpha}}e^{i\phi_0}. \tag{2.10}$$

As $R - R_{l.b.} \to \infty$ on the inner scale, Eq. (2.10) yields

$$\begin{aligned} u^*_{TS}/u^*_{ac} \to\; & 2A_{l.b.}\,e^{2i\alpha_{TS}(R_{l.b.})(R-R_{l.b.})+i\alpha'_{TS}(R-R_{l.b.})^2} \\ & - \frac{R_{h_0}}{R_{l.b.}}\,\frac{\Lambda_u(R_{l.b.})}{i\sqrt{2\pi}\,D_\alpha(R - R_{l.b.})}\,e^{i\phi_0+2i\alpha_{TS}(R_{l.b.})(R-R_{l.b.})+i\alpha'_w(R-R_{l.b.})^2}\,, \end{aligned} \tag{2.11}$$

implying that the disturbance motion downstream of the inner region is dominated by the homogeneous (i.e., the instability wave) solution, which is larger in amplitude than the particular solution (2.7a) by a factor of at least $(R - R_{l.b.})\sqrt{D_\alpha} = O(R^{3/8}_{l.b.})$; see Fig. 3. The effective coupling coefficient in the perfectly synchronous case is then given by

$$C_{p.s.}(R) = 2A_{l.b.} = \frac{R_{h_0}}{R_{l.b.}}\sqrt{\frac{2}{iD_\alpha}}\,\Lambda_u(R_{l.b.})\,e^{i\phi_0}, \tag{2.12}$$

which is identical to the steepest-descent result (2.6). The reader may note that, since the coupling coefficient was determined entirely by the solution in the shorter inner region, nonparallel effects associated with the streamwise derivatives of the base flow, and the vertical velocity associated with the same, can be neglected to the leading order, at least.

2.2.2 Near resonant geometries: the effect of detuning

Other types of near-resonant geometries, corresponding to arbitrary modulation of the waviness amplitude on the length scale of the resonance region, can also be handled in a manner similar to that

in Section 2.2.1 above. Thus, for geometries of the form $h_w = A_w(R)e^{2i\alpha_{TS}(R_{l.b.})(R-R_{l.b.})}$, with $A_w(R)$ varying on the inner scale, one obtains

$$A(R) = A_{l.b.}e^{i\alpha'_{TS}(R-R_{l.b.})^2} + \sqrt{\frac{2}{\pi}}\,\frac{R_{h_0}}{R_{l.b.}}\,\Lambda_u(R_{l.b.})\,e^{i\alpha'_{TS}(R-R_{l.b.})^2}\int_{R_{l.b.}}^{R} A_w(R_s)\,e^{i\alpha'_{TS}(R_s-R_{l.b.})^2}dR_s. \quad (2.13)$$

For the case of spatially periodic geometries with a wavenumber detuning of α_{w_1} with respect to $\alpha_{TS}(R_{l.b.})$, i.e.,

$$A_w(R) = e^{2i\alpha_{w_1}(R-R_{l.b.})+i\phi_0}, \quad (2.14a)$$

this leads to

$$C(\alpha_{w_1}) = e^{\frac{\alpha_{w_1}^2}{iD_\alpha}}\,C_{p.s.}, \quad (2.14b)$$

indicating that the effective coupling coefficient due to an individual Fourier component drops off in a gaussian manner away from the resonant wavenumber $\alpha_{l.b.}$. By observing that only the real part of iD_α contributes to the magnitude of the exponential factor, it is clear that this drop-off is purely due to the streamwise variation in the instability growth rate near $R = R_{l.b.}$. Basically, if one views the phase-synchronization process in terms of the real parts of the respective wavenumbers (α_w and α_{TS}), then, for the detuned cases, the center of the resonance region is somewhat upstream or downstream of the lower branch location, which implies a reduced amplification ratio between the resonance region and the upper branch, and in turn, a reduced magnitude of the effective coupling coefficient. Only a detuning of up to $\alpha_{w_1} = O(\sqrt{D_\alpha})$, corresponding to $\alpha_{w_1}/\alpha_{TS}(R_{l.b.}) = O(R_{l.b.}^{-3/8})$, can produce any significant receptivity, due to the scaling of $\Delta R/R_{l.b.} = O(R_{l.b.}^{-3/8})$ for the resonance region.

Figure 4 shows the magnitude of the normalized effective coupling coefficient, $C(\alpha_{w_1})/R_{h_0}$, plotted as a function of the wavenumber detuning parameter $\alpha_{w_1}/\alpha_{TS}(R_{l.b.})$ expressed as a percentage, for two different values of the frequency parameter $f = \omega^*\nu^*/U_\infty^{*2}$. The frequency of $f = 25 \times 10^{-6}$ has a logarithmic amplification factor of about 9, and, hence, lies in the most critical range of frequencies for the transition process. On the other hand, the frequency of $f = 55 \times 10^{-6}$, although not very important for transition, may be relevant to laboratory experiments. The figure shows that the analytical predictions at both frequencies are in very good agreement with the results obtained from a numerical solution of the wave amplitude equation (2.2). The only significant difference between the two results appears to be that, at large positive values of the detuning parameter (> 8%), the numerical coupling coefficient decreases more slowly than the gaussian drop-off predicted in the analytical solution (2.14b).

2.3 Geometries with a continuous spectrum of a deterministic or random nature

Now, consider the class of surface imperfections which have a continuous spatial spectrum, and, therefore, cannot be classified as discrete-mode waviness. Assuming the spectrum to be homogeneous in the streamwise direction, one can integrate over all contributions of the form (2.14b) in order to arrive at the total coupling coefficient for any particular geometry. In addition to its dependence on the power spectral density $R^2_{h_0}(\alpha_{w_1})$ of the surface-irregularity distribution, the coupling coefficient also depends upon the relative phase distribution, $\phi_0(\alpha_{w_1})$, between the different wavenumber components of the surface undulations. However, an obvious conclusion that holds for all geometries with a continuous spatial spectrum is that the integrated coupling coefficient is $O(R_{l.b.}^{-5/8})$ times smaller than the discrete mode solutions (2.12) and (2.14a), since the bandwidth in the α_w space which can contribute significantly to this integral is only of $O(R_{l.b.}^{-5/8})$. This makes the overall receptivity even smaller than that induced by an isolated roughness element with a comparable perturbation in height. Note that the receptivity is stronger for the discrete mode waviness of the form (2.3), because the latter represents a peak in the spatial spectrum of the surface irregularity near the resonant wavenumber, and, thus, posseses more *energy* in the relevant band of wavenumbers.

Lacking a precise knowledge about the surface irregularities, it is not an easy matter to characterize the phase distribution of the spectral representation of any stationary process. Only a few limited results exist for finite-dimensional distributions [14]; these prove that the phase ϕ_0 at any wavenumber is always uniformly distributed on $[-\pi, \pi]$ and that the joint distributions of the phase variables are independent of the spectral amplitudes. Assuming that this result also holds in the limiting case of a continuous spectrum, and that the corresponding power spectral density $R^2_{h_0}$ does not vary significantly over the narrow bandwidth of the spectrum, one finds that the expected value $< C^2 >^{1/2}$ for an ensemble of rough surfaces which are statistically similar is given by

$$< C^2 >^{1/2} = \sqrt{2\pi}\frac{R_{h_0}}{R_{l.b.}} |sin\,(arg(D_\alpha))\ \Lambda_u(R_{l.b.})|\,, \tag{2.15}$$

where *arg* denotes the argument of a complex valued quantity. In any given realization, the effective coupling coefficient will vary from a minimum value of zero to a maximum of $2^{3/4}$ times the average value in (2.15). This upper limit is associated with that particular realization for which contributions from all wavenumbers are in phase, and, therefore, the respective magnitudes can be added to each other in a linear fashion.

3 Concluding Remarks

The theory presented in this paper elucidates the nature of the distributed receptivity process, and provides a closed form approximation for the instability-wave amplitude as a function of the amplitude and frequency of the free-stream disturbance. Although analyzed in the specific context of receptivity due to distributed surface irregularities, the results obtained can be easily generalized to receptivity due to other forms of surface disturbances, such as wall suction, wall admittance/compliance, and wall temperature, etc. An especially important application would be to predict the generation of stationary cross-flow vortices due to distributed surface roughness/suction by generalizing the localized receptivity results obtained earlier [15].

The theory also demonstrates the increased effectiveness of near-resonant forcing, which leads to continual receptivity over long distances. At low speeds, such resonant forcing can only be produced via the interaction of the free-stream disturbances with surface inhomogeneities of different types, such as surface roughness, short-scale variations in suctions, etc. However, in supersonic flows, phase speeds of the free-stream and boundary-layer disturbances are of the same order, and a near-resonant forcing could possibly arise directly, without any need for "tuning" via scattering at the boundary surfaces. If such an unsteady forcing does indeed occur, the ideas presented above might turn out to be applicable in predicting the boundary-layer response in these problems as well. Our current effort is focussed along this direction.

Acknowledgements

Financial support for this work was provided by the Theoretical Flow Physics Branch, Fluid Mechanics Division, NASA Langley Research Center, Hampton, VA, under contract NAS1-18240. The author would like to acknowledge some useful discussions with Drs. Sharath Girimaji and Surya Dinavahi. Efforts of Drs. Craig Streett and James Townsend in reviewing the manuscript are also appreciated.

References

[1] Braslow, A. L. and Fischer M. C., "Design Cosiderations for Application of Laminar Flow Control Systems to Transport Aircraft," AGARD-R-723, pp. 4.1-4.27, 1985.

[2] Goldstein, M. E., "Scattering of Acoustic Waves into Tollmien-Schlichting Waves by Small Streamwise Variations in Surface Geometry," *J. Fluid Mech.*, Vol. 154, pp. 509-529, 1985.

[3] Ruban, A. I., "On the Generation of Tollmien-Schlichting Waves by Sound," Transl. in *Fluid Dyn.*, Vol. 19, pp. 709-16, 1985.

[4] Chen, C. F., ed., "Mechanics USA 1990," Proc. 11th US Natl. Cong. Appl. Mech., Tucson, Arizona, May 1990.

[5] Reda D. C., Reed, H. L. and Kobayashi, R., eds., "Boundary Layer Stability and Transition to Turbulence," FED-Vol. 114, ASME, N.Y., pp. 63-68, 1991.

[6] Crouch J. D., "A Nonlinear Mode Interaction Model for Boundary Layer Receptivity," *Bull. APS*, Vol. 35, No. 10, p. 2262, 1990.

[7] Crouch J. D., "Initiation of Boundary-Layer Disturbances by Nonlinear Mode Interactions," Boundary Layer Stability and Transition to Turbulence, Ed. Reda *et al*, FED-Vol. 114, ASME, N.Y., pp. 63-68, 1991.

[8] Choudhari, M., and Streett, C. L., "A Finite Reynolds Number Approach for the Prediction of Boundary Layer Receptivity in Localized Regions," NASA TM-102781, Jan. 1991.

[9] Tam, C. K. W., "The Excitation of Tollmien-Schlichting Waves in Low Subsonic Boundary Layers by Free-Stream Sound Waves," *J. Fluid Mech.*, Vol. 109, pp. 483-501, 1981.

[10] Choudhari, M., "Distributed Acoustic Receptivity in Laminar Flow Control Configurations," NASA CR-4438, May 1992.

[11] Ackerberg and Phillips, "The Unsteady Laminar Boundary Layer on a Semi-infinite Flat Plate due to Small Fluctuations in the Magnitude of the Free-Stream Velocity," *J. Fluid Mech.*, Vol. 51, pp. 137-157, 1972.

[12] Kevorkian, J., "Perturbation Techniques for Oscillatory Systems with Slowly Varying Coefficients," *SIAM Rev.*, Vol. 29, No. 3, pp. 391-462, 1987.

[13] Kevorkian, J., "Passage through Resonance for a One-Dimensional Oscillator with Slowly Varying Frequency," *SIAM J. Appl. Math.*, Vol. 20, p. 364, 1971.

[14] Kimme, E. G., "Distributions of Phases of Sinusoidal Components of Ergodic Trigonometric Series," *SIAM Rev.*, Vol. 7, No. 1, pp. 88-99, 1965.

[15] Choudhari, M., and Streett, C. L., "Boundary Layer Receptivity Phenomena in Three-Dimensional and High-Speed Boundary Layers," AIAA Paper 90-5258, 1990.

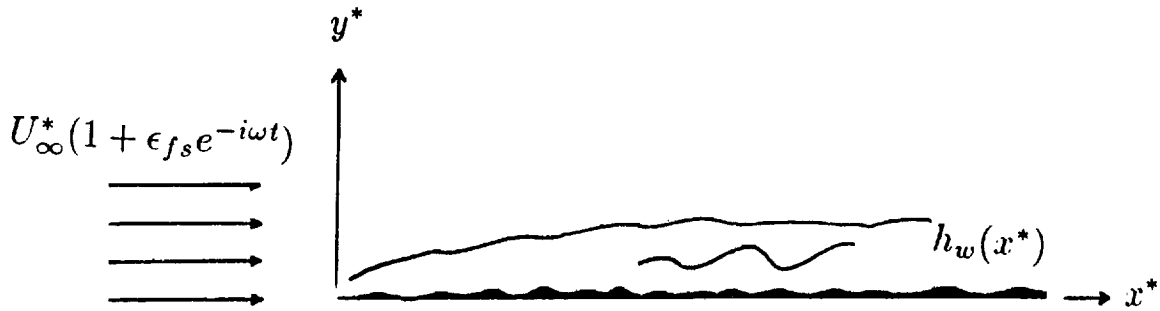

Fig. 1 Sketch of the problem.

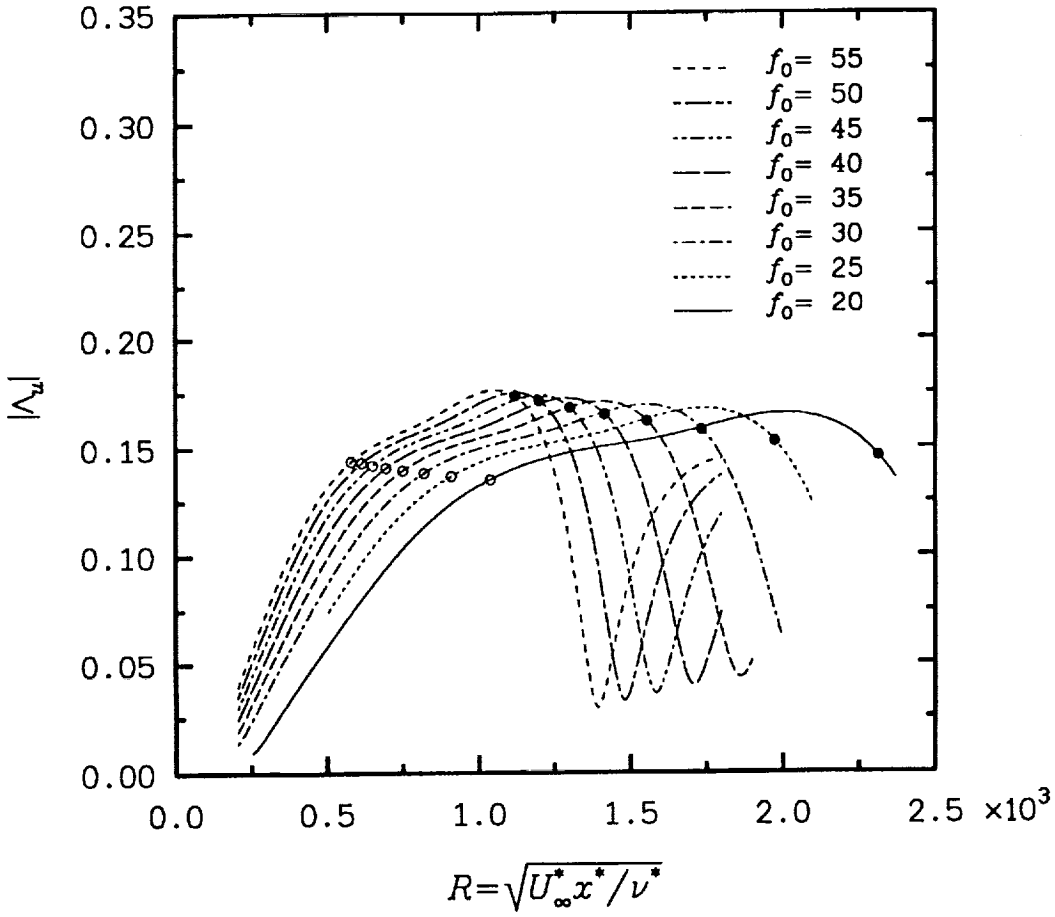

Fig. 2 Magnitude of the efficiency factor Λ_u from Eq. (2.1a) as a function of the wall inhomogeneity location R with $f_0 = 10^6 \times \omega^* \nu^* / U_\infty^{*2}$ as a parameter. The lower- and upper-branch neutral locations at each frequency are indicated by open and filled circles, respectively.

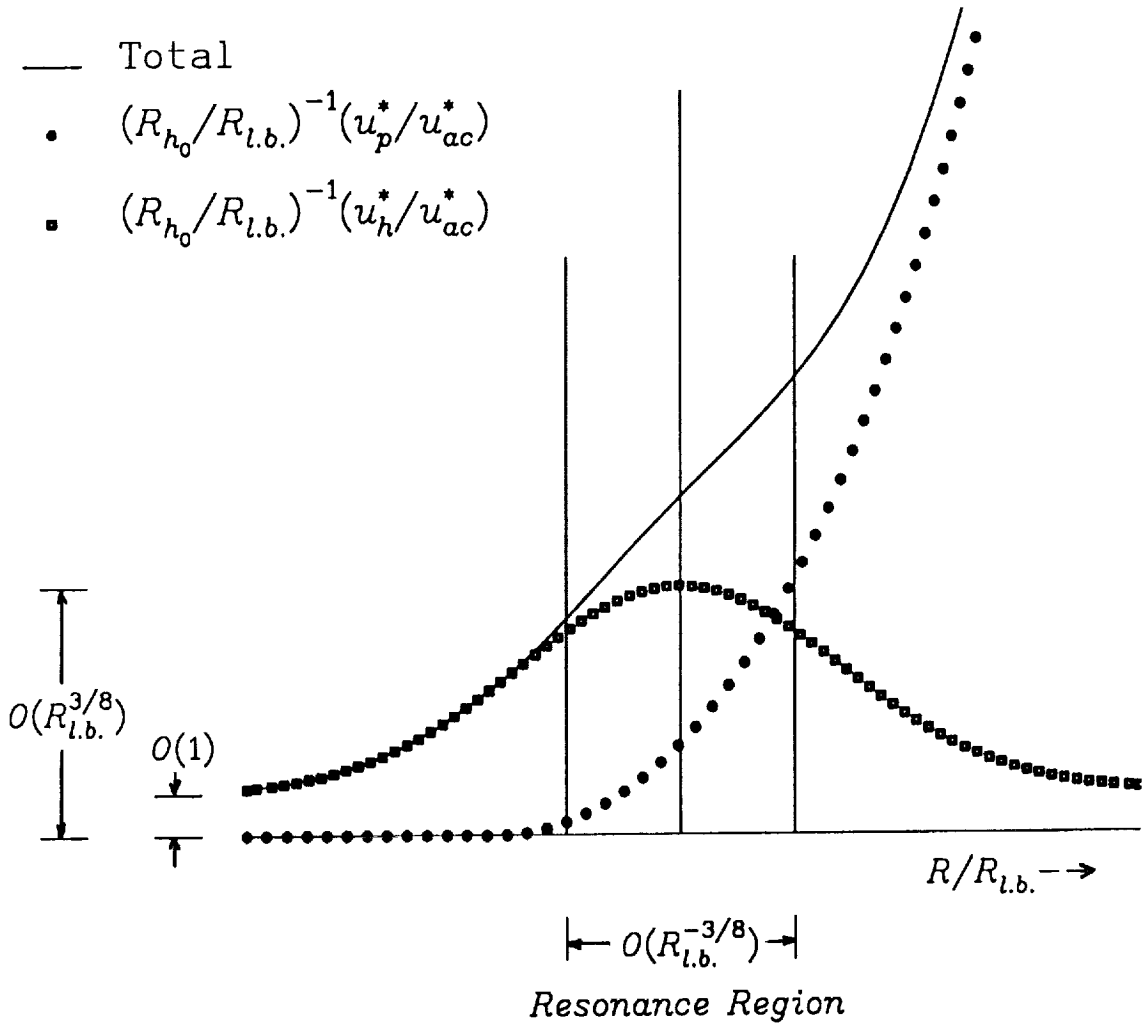

Fig. 3 A sketch of the development of the wave amplitude across the resonance region. Note that the decomposition of the solution between the particular and homogeneous components inside the resonance region is purely imaginary, and has been shown for the purpose of intuitive understanding only.

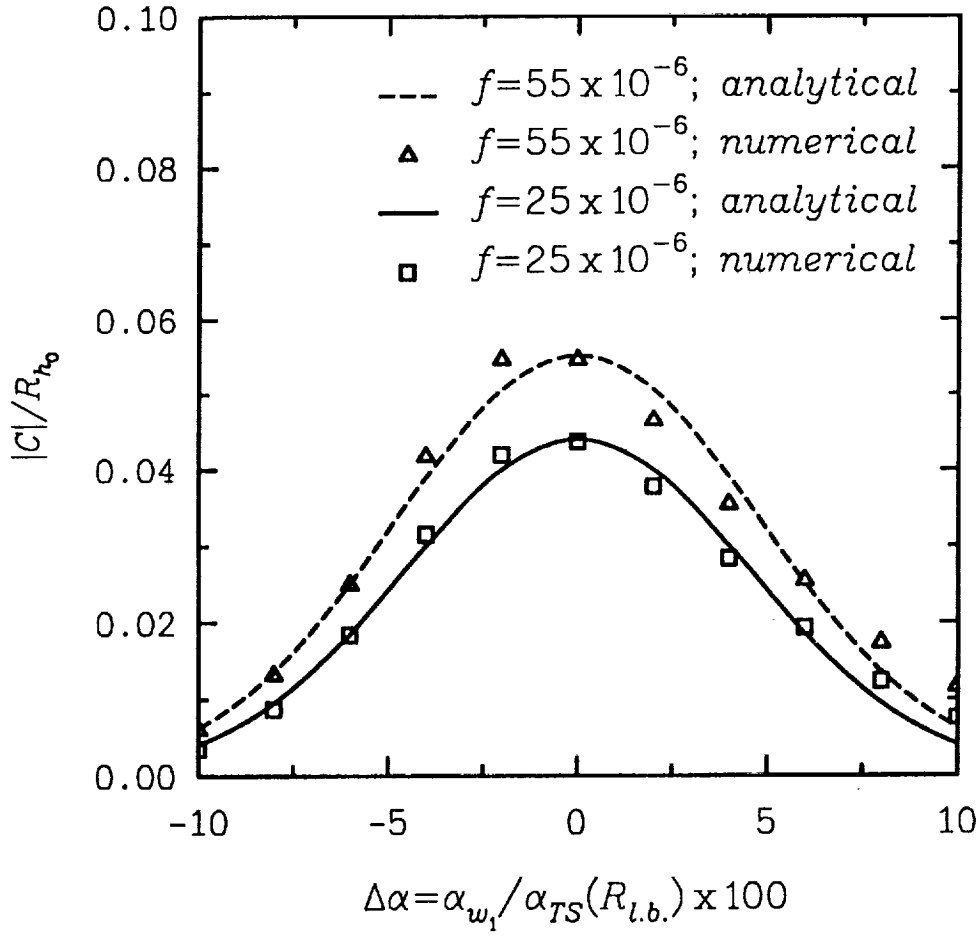

Fig. 4 Receptivity induced by discrete-mode surface waviness: the normalized effective coupling coefficient, $|C|/R_{h_0}$, as a function of the wavenumber detuning parameter $\Delta\alpha=\alpha_{w_1}/\alpha_{TS}(R_{l.b.})\,x\,100$

REPORT DOCUMENTATION PAGE

Form Approved
OMB No. 0704-0188

1. AGENCY USE ONLY (*Leave blank*)	2. REPORT DATE	3. REPORT TYPE AND DATES COVERED
	May 1992	Contractor Report

4. TITLE AND SUBTITLE
Boundary-Layer Receptivity Due to Distributed Surface Imperfections of a Deterministic or Random Nature

5. FUNDING NUMBERS
C NAS1-18240

WU 537-03-23-03

6. AUTHOR(S)
Meelan Choudhari

7. PERFORMING ORGANIZATION NAME(S) AND ADDRESS(ES)
High Technology Corporation
28 Research Drive
Hampton, VA 23666

8. PERFORMING ORGANIZATION REPORT NUMBER

9. SPONSORING / MONITORING AGENCY NAME(S) AND ADDRESS(ES)
National Aeronautics and Space Administration
Langley Research Center
Hampton, VA 23665-5225

10. SPONSORING / MONITORING AGENCY REPORT NUMBER
NASA CR-4439

11. SUPPLEMENTARY NOTES
Langley Technical Monitor: Craig L. Streett
Final Report

12a. DISTRIBUTION / AVAILABILITY STATEMENT
Unclassified-Unlimited

Subject Category 34

12b. DISTRIBUTION CODE

13. ABSTRACT (*Maximum 200 words*)

Acoustic receptivity of a Blasius boundary layer in the presence of distributed surface irregularities is investigated analytically. It is shown that, out of the entire spatial spectrum of the surface irregularities, only a small band of Fourier components can lead to an efficient conversion of the acoustic input at any given frequency to an unstable eigenmode of the boundary layer flow. The location, and width, of this most receptive band of wavenumbers corresponds to a relative detuning of $O(R_{l.b.}^{-3/8})$ with respect to the lower-neutral instability wavenumber at the frequency under consideration, $R_{l.b.}$ being the Reynolds number based on a typical boundary-layer thickness at the lower branch of the neutral stability curve. Surface imperfections in the form of discrete mode waviness in this range of wavenumbers lead to initial instability amplitudes which are $O(R_{l.b.}^{3/8})$ larger than those caused by a single, isolated roughness element. In contrast, irregularities with a continuous spatial spectrum produce much smaller instability amplitudes, even compared to the isolated case, since the increase due to the resonant nature of the response is more that compensated for by the asymptotically small band-width of the receptivity process. Analytical expressions for the maximum possible instability amplitudes, as well as their expectation for an ensemble of statistically irregular surfaces with randon phase distributions, are also presented.

14. SUBJECT TERMS
Receptivity, Transition, Boundary Layers

15. NUMBER OF PAGES
18

16. PRICE CODE
A03

17. SECURITY CLASSIFICATION OF REPORT	18. SECURITY CLASSIFICATION OF THIS PAGE	19. SECURITY CLASSIFICATION OF ABSTRACT	20. LIMITATION OF ABSTRACT
Unclassified	Unclassified		

NSN 7540-01-280-5500

Standard Form 298 (Rev. 2-89)
Prescribed by ANSI Std. Z39-18
298-102

NASA-Langley, 1992